MADRID
inter.noise 2019
June 16 - 19
NOISE CONTROL FOR A BETTER ENVIRONMENT

Flyover Noise of Multi-Rotor sUAS

Alexander, W. Nathan[1]
Virginia Tech
Kevin T. Crofton Department of Aerospace and Ocean Engineering
Center for Research in Experimental Aero/Hydrodynamic Technology (CREATe)
McBryde Hall, Room 660
225 Stanger St.
Blacksburg, VA 24061

Whelchel, Jeremiah[2]
Virginia Tech
Kevin T. Crofton Department of Aerospace and Ocean Engineering
Center for Research in Experimental Aero/Hydrodynamic Technology (CREATe)
McBryde Hall, Room 660
225 Stanger St.
Blacksburg, VA 24061

ABSTRACT

Drone delivery and urban air mobility concepts often employ multi-rotor VTOL configurations. These vehicles are designed to operate within urban environments potentially exposing communities to significant levels of tonal and broadband noise. Acoustic regulations or operational guidelines do not exist to minimize the impact of these flights on surrounding communities. Recent work at Virginia Tech is focused on understanding the noise produced by these platforms in-flight, particularly during maneuver, and its impact on ground observers. Acoustic measurements of multi-copter drone flyovers have been conducted in the drone park at Virginia Tech including the basic maneuvers of hover and forward flight. Three distinct frequency regions are identified in the sound spectra relating to the tonal noise, broadband interaction noise, and rotor self-noise. Comparison of the noise produced in hover and forward flight reveals the influence of directivity on the measured sound at a receiver and should be accounted for in estimates of community impact.

Keywords: sUAS, Flyover, Drones
I-INCE Classification of Subject Number: 13

1. INTRODUCTION

Commercial and recreational multi-rotor drones, or sUAS, are increasingly popular but produce considerable noise. The proximity of these drones to communities increases the potential of population annoyance in areas previously not subjected to

[1] Assistant Professor, alexande@vt.edu
[2] Graduate Research Assistant, jwhelche@vt.edu

aircraft noise. Additionally, qualities of the noise produced by these platforms have been shown to be particularly annoying. Christian and Cabell[1] conducted psychoacoustic experiments comparing the sound of drones to typical ground vehicles in residential communities. Their results suggest that subjects may be more disturbed by the noise from sUAS than typical road vehicles at equivalent standard metric levels: SEL_A, SEL_C, EPNL, and L_5.

The total noise produced by these platforms is a combination of various aerodynamically generated sources. Broadband sources include separation noise, trailing edge noise, body/propeller, and propeller/propeller interaction noise. Tonal sources also exist generated by steady loading and thickness noise. Previous theoretical and experimental studies concerning large rotorcraft have shown that blade thickness noise propagates primarily in the blade disk while loading noise, steady and unsteady, propagates normal to the blade disk. Trailing edge noise and other scattered broadband sources can propagate both in the disk plane and normal to the rotor disk.

Regulators are beginning to address the environmental impact of drones on communities including noise pollution. The European Union Aviation Safety Agency (EASA) has recently published a proposal to regulate the noise produced by drones[2]. Therefore, a fair and accurate method of determining the community annoyance needs to be determined. This begins with correctly estimating the noise of different platforms through various phases of flight.

The objective of this study is to compare the noise produced by a drone in a static (hover) flight condition to forward free flight. These results are intended to aid the development of community noise tools for sUAS as well as proposed urban air mobility (UAM) multi-rotor concepts. A DJI Matrice 600 Pro was chosen for this study as it is a large recreational drone that can handle a payload size comparable to that needed for package delivery applications. Noise sources are identified through spectral analysis of these data. Additionally, integrated values of acoustic pressure are compared between hover and flyover. Results show that the measured noise is a strong function of receiver angle and distance from the source. Thus, directionality should be considered when estimating community impact.

2. EXPERIMENTAL SET-UP

2.1 Virginia Tech Drone Park

All measurements were conducted in the Virginia Tech Drone Park. The drone park is an on-campus outdoor netted facility designed for free flight sUAS research. The park, operated by the Mid-Atlantic Aviation Partnership (MAAP), opened in early 2018 as the tallest netted drone research facility in the US with dimensions 25.9 m tall, 91.4 m long, and 36.6 m wide. The floor of the park is an unpaved but maintained grass field. Flights were conducted in the drone park, Figure 1, along the longest dimension with ground microphones positioned spanwise across the flight path at the midpoint of the park.

2.2 Drone and Flight Instrumentation

A DJI Matrice 600 Pro hexacopter was used for this study, shown in Figure 2. This is a popular recreational drone with a considerable maximum take-off weight of 148.1 N representative of platforms that could be used for drone delivery services. It has a maximum forward flight speed of 18 m/s. The drone has six two-bladed DJI 2170R propellers with a diameter of 533.4 mm and pitch of 178 mm. The drone position was maintained and logged at a rate of 10Hz using the on-board A3 Pro controller system with

three GPS units and IMU's for triple redundancy and a barometer. These data were synced with acoustic measurements using a separate GPS unit recording the GPS time simultaneous with microphone measurements. Therefore, position data are accurately synchronized with acoustic measurements within 0.10 s.

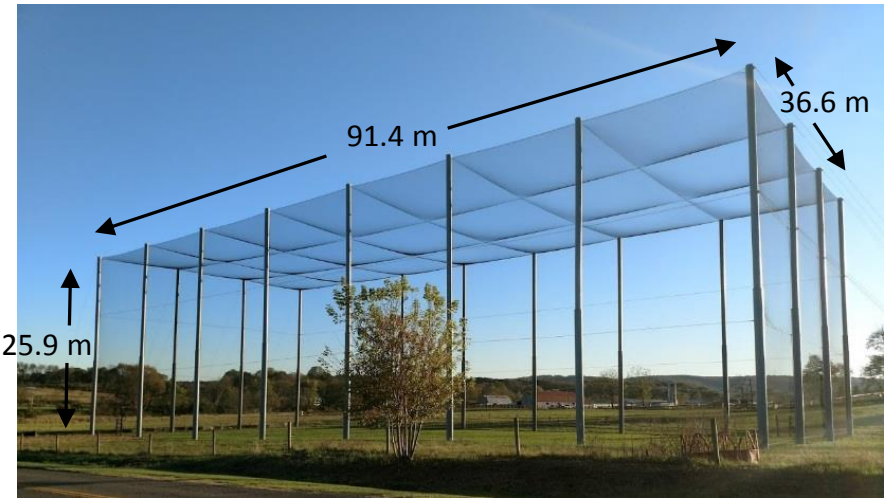

Figure 1. Virginia Tech Drone Park

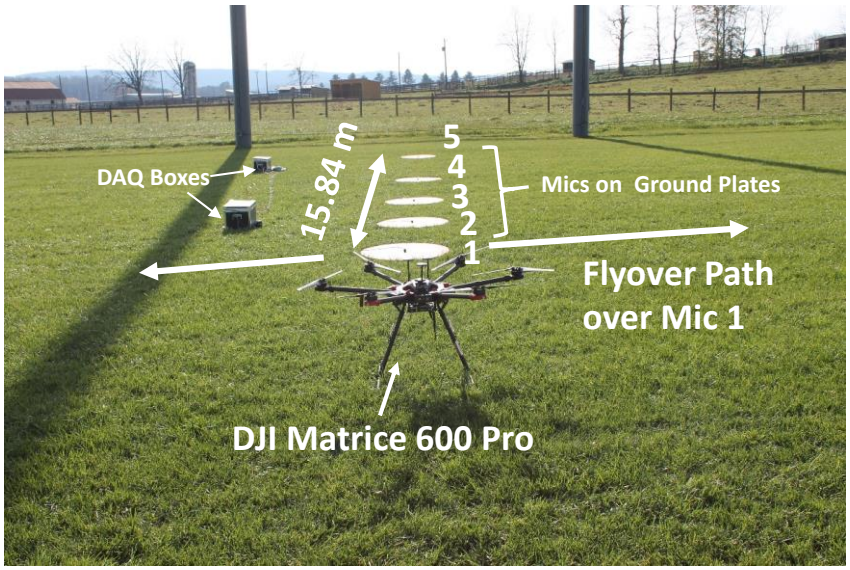

Figure 2. DJI Matrice 600 Pro drone and ground microphone instrumentation

2.3 Microphones and Data Acquisition

Five Bruel & Kjaer 4190 ½" microphones were used to measure the noise from the drone. These microphones were positioned at the center of 1 m diameter by 1.3 cm thick HPVA maple plywood ground plates. The spanwise relative location of each microphone is described by Figure 3 and Table 1. Mic 1 was nominally directly under the flight path of the vehicle. The microphones were positioned on their side pointing towards the Mic 1 location. Mic 1 was positioned on its side pointing in the same direction. All microphones used wind screens to reduce background noise. Data were acquired with synchronized Bruel & Kjaer LAN-XI Type 3050 data acquisition modules sampling at 65536 Hz. All spectral data were processed with record lengths of 6555, 0.1 ms, for a consistent frequency resolution of approximately 10 Hz.

Environmental conditions were recorded with a weather station located at the drone park. All presented measurements were conducted on the same day, Nov. 18th, 2018, within a period of an hour and a half. Environmental conditions remained constant over this time at 10°C, < 1 knot steady wind with gusts to 4.3 knots, and 70% humidity.

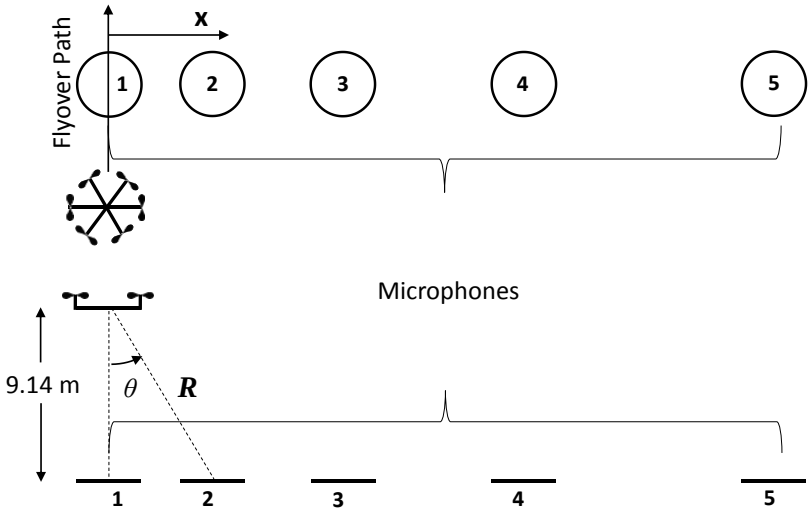

Figure 3. Nominal flight path and microphone configuration

Table 1. Mic locations and positions relative to nominal flight path

Mic #	Spanwise Location x, m	θ_{min}, degrees	R_{min}, m
1	0	0	9.14
2	2.45	15	9.46
3	5.28	30	10.56
4	9.14	45	12.93
5	15.84	60	18.29

3. RESULTS

3.1 Flyover Noise

The time series acoustic pressure for a single flyover as measured by each of the five ground microphones is shown in Figure 4 for a flyover altitude of 7.5 m. The noise increases as the drone passes directly across the spanwise location of the microphones. The ground speed of the vehicle is overlaid on the time series for Mic 1 as well. The average speed for the central 14s period of flight is approximately constant with an average of 3.23 m/s. Although the maximum speed of the drone is 18 m/s, the speed of the drone in these flights was limited by the length of the cage.

Sound Exposure Level (SEL) is a common metric used to characterize transient events like the disturbance produced by an aircraft flyover. It represents the acoustic level required to produce the same amount of energy as the transient event over a period of 1s and is calculated as in Equation 1. The SEL in dB(Z) for the drone flyover was computed for this event by integrating the squared acoustic pressure over the 14s period for which the vehicle speed was constant. SEL for each microphone is given in Table 2.

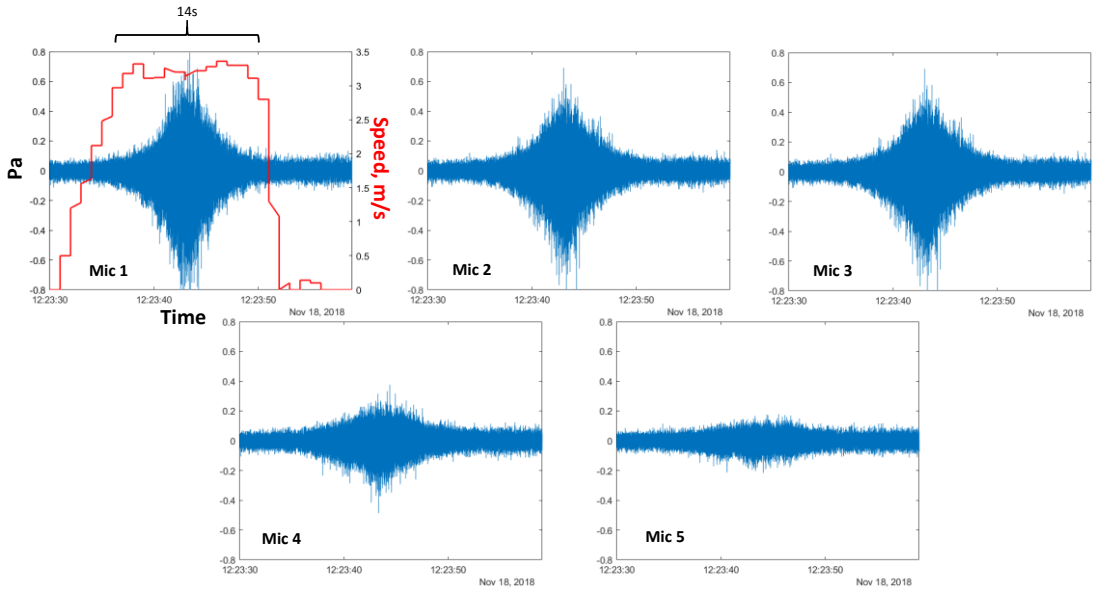

Figure 4. Flyover acoustic pressure time history for all five microphones for a drone altitude of 7.5 m and forward speed of 3.23 m/s

$$SEL = 10\,log_{10}\left(\frac{\int_{t_1}^{t_2} p(t)^2 dt}{(20\mu Pa)^2}\right) \qquad \textit{Equation 1.}$$

Table 2. Sound Exposure Level for 7.5 m altitude and 3.23 m/s flyover

	Mic 1	**Mic 2**	**Mic 3**	**Mic 4**	**Mic 5**
dB(Z)	85.3	84.0	82.7	79.6	75.9

Spectrograms of the noise measured by Mic 1 are shown in Figure 5. These spectrograms are calculated with a time resolution of 0.10s. Figure 5(a) shows the spectrogram for the full measurement period. The measurement begins with the drone in operation on the ground. As the drone increases altitude prior to the flyover, the measured broadband noise above 1 kHz increases. Forward flight begins at approximately 12:23:30 (hh:mm:ss). At this point, tones between the second and fifth harmonic of the blade passage frequency noticeably shift frequency as the rotor blades change rotational speeds. The period of constant drone ground speed is shown between the two dashed lines. Figure 5(b) is the same spectrogram with limits defined by this period of constant forward speed. A dashed black line indicates the moment in which the drone is directly overhead as measured by GPS. This point is approximately 0.3s behind the noise peak in the spectrogram. The peak noise from helicopter rotors tends to project forward, but this is primarily a result of BVI noise unlike the broadband signature observed in the drone spectrum. Instead, unsteady loading broadband noise tends to have a dipole directivity which peaks below the rotor disk plane[3,4]. The observed shift is more likely due to uncertainty of the GPS location and the accuracy of the synchronized acoustic and GPS signals.

As the drone approaches the microphones the strength of the blade passage frequency tone and its harmonics increase, but the peak frequency of each tone remains fixed. Zawodny *et al.*[5] present similar spectrograms of flyovers for a DJI Phantom 2 and

a Prioria Hex. Their data are limited to frequencies below 1 kHz, but they show rotor tones dominate the noise spectrum in this frequency range. They also show significant wandering of these rotor tones with time. The broadband noise shown in Figure 5(b) changes in both amplitude and frequency. There are two regions of significant broadband noise. The mid-frequency region extends from 300 Hz to 5 kHz. A second higher frequency region extends from 5 kHz to 20 kHz. The peak frequencies in both regions vary as the drone passes the microphone. The peak frequencies shift lower as the receiver angle, θ, nears zero. The high frequency region has a single hump, although the sound pressure level may rise again at frequencies beyond 20 kHz. The mid-frequency region is composed of several humps all changing peak frequency with drone position.

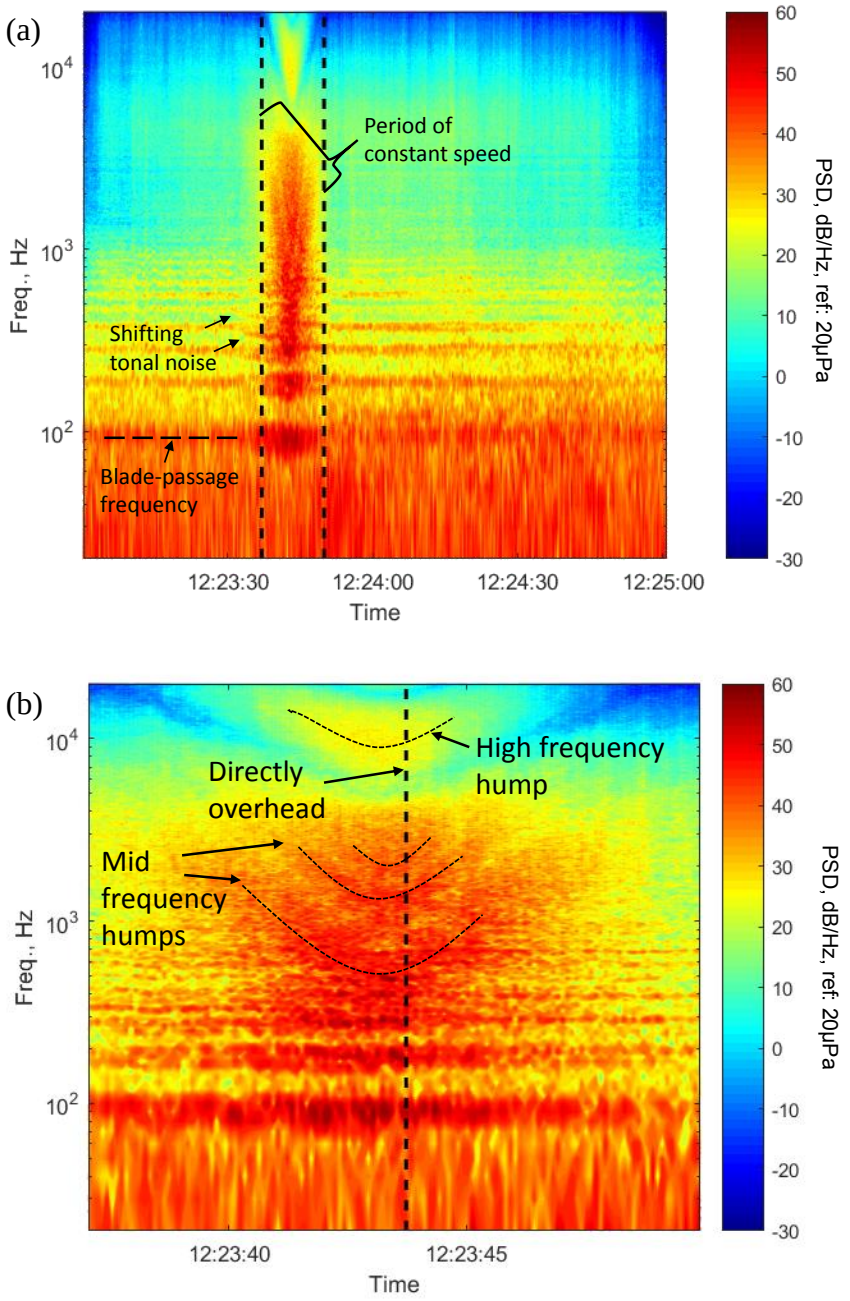

Figure 5. Spectrogram of measurement at Mic 1 for flyover at 7.5 m at 3.23 m/s (a) full time series (b) and period of constant flight speed

Narrowband power spectral density are computed from these spectrograms by averaging over time. Figure 6 shows a 12s and narrower 2s average of these data centered about the point at which the drone is directly overhead. The spectra are dominated by the rotor BPF tones and harmonics from ~100 Hz to 700 Hz. The rotors are not synchronized and do not spin at the same RPM so these tones are scattered which is particularly noticeable at higher harmonics ($n \geq 3$). The broadband humps at mid and high frequencies are evident above this low frequency region. Averaging over a smaller period of time (2s) reduces the spectral smoothing created by averaging over the spectral features which shift and change magnitude with time. The 2s average spectrum has a stronger high frequency hump and some scalloping is apparent in the mid-frequency region between 1 kHz-3kHz. Of course, these characteristics are also obscured by the increasing uncertainty due to the lower number of spectral averages.

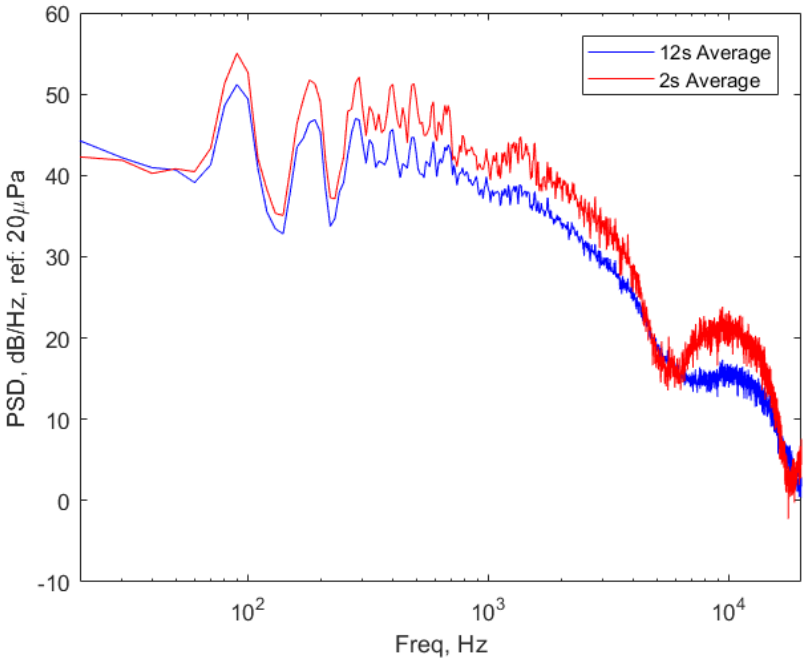

Figure 6. Average spectra for 7.5 m/s and 3.23 m/s flyover

3.2 Hovering Noise

Measurements were also conducted with the drone in hover directly above Mic 1. The drone was at a constant altitude of 9.18 m above the microphone. The spectrogram for Mic 1 is shown in Figure 7. Figure 8 shows the spectrogram for Mic 5 at the same condition. Mic 5 is at a spanwise receiver angle, θ = 60°, from a position directly below the drone. The drone's operation is steady in this condition such that the peak of the rotor related tones do not wander across frequency like observed in Cabell *et al.*[6] for the DJI Phantom 2 and Prioria Hex at similar altitude.

Since these data are constant with respect to time, the spectra are more easily compared through time-averaged frequency spectra as shown in Figure 9. The BPF and harmonics are visible in all spectra up to approximately 1 kHz. The strength of these tones decreases with increasing distance from the drone. Above 1 kHz, the tones diminish into the broadband noise. The spectral shape of the broadband noise changes significantly with position. At Mic 1, directly under the drone, the spectrum has lumps from 1 kHz and 3 kHz spaced approximately 600 Hz apart peak-to-peak. At Mic 2, slightly displaced from the center of drone body, these lumps decrease in magnitude and the peaks shift to slightly higher frequency. This trend continues with increasing receiver angle, θ. The high

frequency broadband noise continues a similar trend. The peak magnitude decreases from Mic 1 to Mic 5 and the peak frequency increases. For Mic 5, the peak frequency shifts beyond 20 kHz, the limit of the figure.

Similar spectral characteristics have been found in acoustic spectra from helicopter rotors. It has been suggested that the mid-frequency noise is associated with unsteady interaction effects for helicopters, typically BVI[7]. In the case of the drone, there may be interaction between adjacent rotors and the drone body which contributes significantly to the unsteady blade loading producing the broader spectral features. The high frequency noise is in the frequency range associated with blade self-noise including sources such as separation noise, turbulent boundary layer trailing edge noise, or laminar boundary layer vortex shedding noise. A static airfoil prediction of these sources using the chord and local blade speed at 75% radius is shown in Figure 9 for reference. This prediction uses the method presented by Brooks *et al.*[8] to produce 1/3rd octave-band spectra. It is assumed that the higher velocity regions in the outer part of the blade disk dominate the self-noise produced by the rotor. At this location the blade has a chord of 22.2 mm. The prediction is completed for a local blade angle of attack of 8° and 4°. The geometric pitch at this radial location is approximately 8°. The pitch angle is an overestimate of the local blade angle of attack because it does not take into account the inflow velocity to the rotor. Thus, a lower value of 4° is used to illustrate the effect of lowering the angle of attack. The absolute value of this prediction has been adjusted for comparison to highlight the similarity in spectral shape. An absolute prediction would require modeling the geometric and velocity variation along the blade span. Nonetheless, the predictions peak in the frequency range of the identified high frequency region suggesting that self-noise sources are the probable dominant sources in this frequency range.

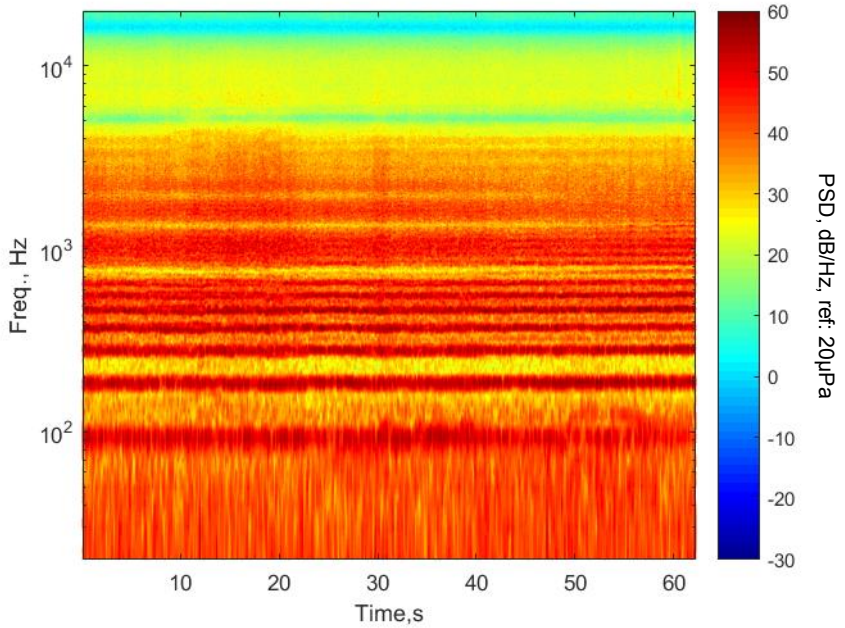

Figure 7. Mic 1 spectrogram for hover at 9.18 m

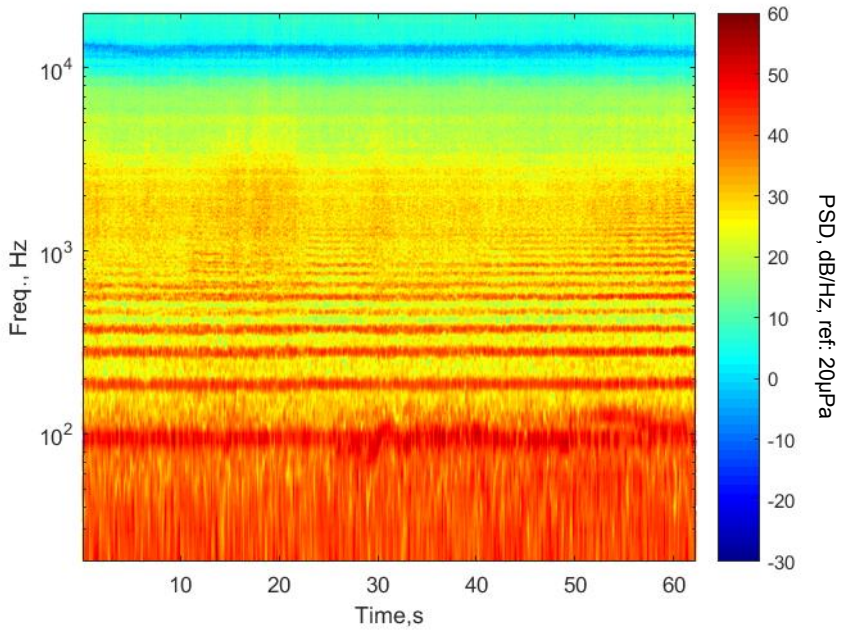

Figure 8. Mic 5 spectrogram for hover at 9.18 m

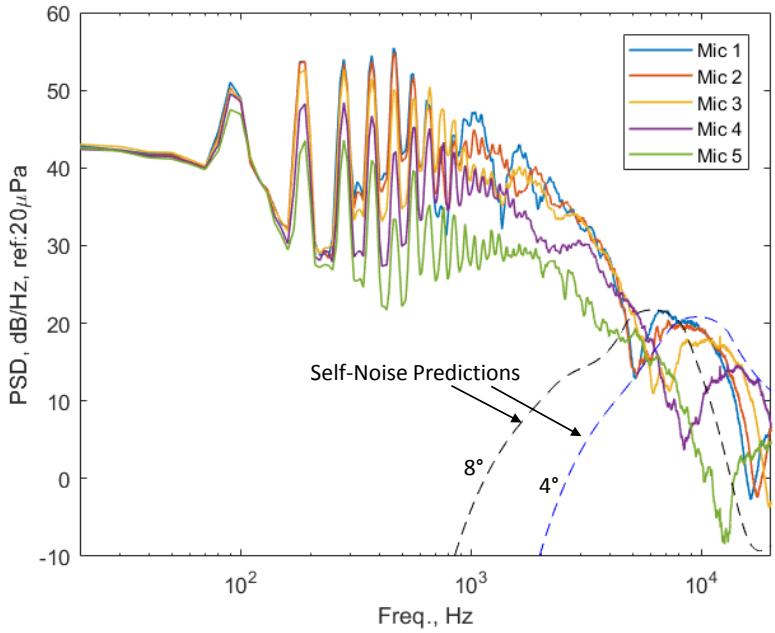

Figure 9. Acoustic frequency spectra for the five microphone positions during hover above Mic 1 at an altitude of 9.18 m

For comparison with the flyover data, SEL can be calculated for the hovering drone by integrating over an equivalent period of time, 14s. Table 3 shows the equivalent SEL for each microphone.

Table 3. Sound Exposure Level for hover at an altitude of 9.18 m

	Mic 1	**Mic 2**	**Mic 3**	**Mic 4**	**Mic 5**
dB(Z)	89.6	88.7	87.3	83.7	79.2

3.3 Comparison of Hover and Flyover

Similar trends are observed in the hover and flyover measurements particularly for the mid and high frequency broadband noise. In the mid and high frequency regions, the broadband peaks in the hover spectra decay and shift to higher frequency from Mic 1 to Mic 5 corresponding to increases in θ and $\boldsymbol{R}$, receiving angle and radial distance. Likewise, during the flyover, the same trends with θ and $\boldsymbol{R}$ are observed. On approach, θ and $\boldsymbol{R}$ decrease reaching a minimum as the drone is directly overhead. At this point, the frequency of the peaks in the broadband noise are at a minimum and their magnitude is a maximum. As θ and $\boldsymbol{R}$ increase for the rest of the flyover, the peak frequencies increase to their initial values and their magnitudes reduce.

Figure 10 is a direct comparison of the Mic 1 and 2 spectra from the hover condition and the 2s spectral average from the flyover. The mid and high frequency regions are similar in magnitude although averaging of the flyover data tends to smooth the lumps particularly in the mid-frequency region. The spectral tones below 1 kHz differ between flyover and hover due to the change in rotor rotational rate during forward flight. All of the rotors do not spin at the same RPM during forward flight. Therefore, the maximum amplitudes of the tones appear weaker, but there are more tones to account for in the flyover spectrum.

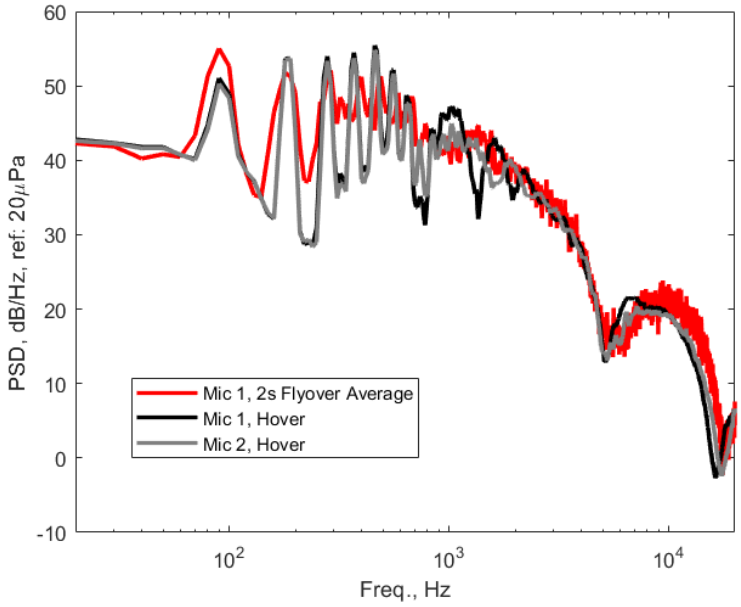

Figure 10. Comparison of spectra from flyover and hover

Differences in calculated SEL given in Tables 2 and 3 are 4.3, 4.7, 4.6, 4.1, and 3.3 dB(Z) for Mics 1 to 5, respectively. In all cases, the calculation of SEL in the hover condition is louder. If the drone noise source is assumed to be a monopole, SEL can be easily calculated for the hover and flyover conditions. The difference between the hover and flyover conditions with this assumption is 2.1 dB at Mic 1 and 1.1 dB at Mic 5. This simple calculation only accounts for the radial decay of noise from the source and the altitude difference between the presented hover and flyover conditions. The observed decrease at all microphones is larger possibly due to the directivity of the drone noise sources.

4. CONCLUSIONS

The noise produced by a DJI Matrice 600 Pro hexacopter was measured during hover and flyover. The presented spectra all have similar qualities corresponding to

spectral features present in three distinct frequency ranges. The low frequency region (<1 kHz) is dominated by tonal noise. The tones give way to broadband noise in the range 1-3 kHz. In this range, the spectra have large humps which are most prominent directly below the drone. At high frequencies, around 10 kHz, self-noise sources dominate. For the presented measurements at a low forward speed, 3.23 m/s, the flyover noise relates well to the noise produced during hover considering the changing directivity and source to receiver distance with respect to time. The amplitude and peak frequency of noise in the mid-frequency and high frequency regions shift with receiver location. The spectra do differ in the low frequency region as the number of separate tones increases due to the variation in rotor rotational speeds in forward flight. Comparison of Sound Exposure Level calculated for the flyover and an equivalent period of hover indicates that the source directivity may significantly influence this metric. Therefore, directivity should be accounted for when estimating the community impact of drone operations.

5. ACKNOWLEDGEMENTS

The authors would like to thank the Institute of Critical Technology and Applied Sciences (ICTAS) at Virginia Tech for their financial support of this work.

6. REFERENCES

1. Christian, A, and Cabell, R, "Initial Investigation into the Psychoacoustic Properties of Small Unmanned Aerial System Noise", 23rd AIAA/CEAS Aeroacoustics Conference, AIAA 2017-4051, (2017)
2. European Aviation Safety Agency, *Opinion No 01/2018: Introduction of a Regulatory Framework for the Operation of Unmanned Aircraft Systems in the 'Open' and 'Specific' Categories*, (2018) from https://www.easa.europa.eu/document-library/opinions/opinion-012018
3. Brooks, TF, Jolly, JR, and Marcolini, MA, "Helicopter Main-Rotor Noise", NASA TP 2825, (1988)
4. Schmitz, FH, "Rotor Noise", *Aeroacoustics of Flight Vehicles*, Ed. Harvey H Hubbard, NASA Reference Publication 1258 vol. 1, TR 90-3052, pp. 65-145, (1991)
5. Zawodny, N, Christina, A, and Cabell, R, "A Summary of NASA Research Exploring the Acoustics of Small Unmanned Aerial Vehicles", AHS Specialists' Conference on Aeromechanics Design for Transformative Vertical Flight, (2018)
6. Cabell, R, McSwain, R, and Grosveld, F, "Measured Noise from Small Unmanned Aerial Vehicles", Proceedings of NOISE-CON 2016, vol. 252, (2016)
7. Blake, WK, "Noise from Rotating Machinery", *Mechanics of Flow-Induced Sound and Vibration, Volume 2*, Elsevier, pp. 505-568, (2017)
8. Brooks, TF, Pope, DS, and Marcolini, MA, "Airfoil Self-Noise and Prediction", NASA Reference Publication 1218, (1989)